Modulational instability in atomic vapors

P. Gauthier,[1] O. Gobert,[2] M. Comte,[1] D. L'Hermite,[1] J. de Lamare,[1] and D. Benisti[1]
[1]*Commissariat à l'Energie Atomique, Centre d'Etudes de Saclay, DEN/DPC/SPAL, 91191 Gif sur Yvette, France*
[2]*Commissariat à l'Energie Atomique, Centre d'Etudes de Saclay, DSM/DRECAM/SPAM, 91191 Gif sur Yvette, France*
(Received 27 September 2001; published 1 March 2002)

We report an experimental, numerical, and analytical study of the near resonant propagation of a laser pulse through an atomic vapor. In the nonlinear regime probed, the light pulse develops frequency sidebands whose positions are, in first approximation, solely dependent on the maximum Rabi frequency of the system, in a fashion very similar to that observed in optical fibers. This modulational instability dictates the temporal reshaping of the laser field and finally results in pulse splitting.

DOI: 10.1103/PhysRevA.65.033834 PACS number(s): 42.65.Sf, 42.50.Md, 42.65.Hw

I. INTRODUCTION

It is well known that the amplitude and phase modulations of a propagating wave may grow in a dielectric medium as a result of an interplay between nonlinear self-phase modulation (SPM) and group-velocity dispersion (GVD). This fundamental process is usually referred to as (temporal) modulational instability (MI). In the frequency domain, MI can be interpreted in terms of a four-wave-mixing (FWM) process: two photons from the pump wave at the frequency ω_L are converted into two different photons, one at the anti-Stokes frequency $\omega_S=\omega_L+\Omega$ and the other at the Stokes frequency $\omega_A=\omega_L-\Omega$, with $2\omega_L=\omega_S+\omega_A$. The first experimental observation of MI in single-mode fibers was reported 15 years ago [1] and since, MI has been recognized as a tool in the field of optical communication to generate solitonlike optical pulses with terahertz repetition rates both in the regimes of normal [2] and anomalous [3] dispersion. In partially stripped plasmas, MI (then referred to as atomic modulational instability, AMI) was also shown to alter the propagation and stability of intense laser pulses [4,5]. AMI requires both bound and free electrons, i.e., the free electrons provide anomalous GVD and bound electrons are responsible for SPM.

In this paper, we report an experimental exhibition of the MI in an atomic vapor, consisting of a collection of two-level atoms. We observed that, due to the nonlinear response of the atoms to the near resonant driving field, the light pulse develops frequency sidebands in the vicinity of $\omega_{MI}=\omega_L \pm \Omega_m/\sqrt{2}$ (where Ω_m is the maximum Rabi frequency of the system) in a fashion very similar to that observed in optical fibers [1,6]. For large propagation distances, this process dictates the temporal reshaping of the laser field and finally results in pulse splitting. Our experimental results (presented in Sec. II) will be shown to be in close agreement with two-dimensional (2D) axisymmetric Maxwell-Bloch (MB) simulations of optical pulse propagation (Sec. III) and will be supported by a perturbative analysis (Sec. IV).

II. EXPERIMENTAL SETUP AND RESULTS

In our experiment, a single-mode stabilized ring dye laser (Coherent 699) pumped by a cw Ar^+ laser was injected into a pulsed dye amplifier composed of three Bethune dye cells [7] pumped transversely by the second harmonic of a single-mode yttrium aluminum garnet:Nd^{3+} laser. The laser was nearly Fourier transform with a full width at half maximum (FWHM) of the power spectral density of the order of 85 MHz. The central wavelength was determined from a measurement of the ring laser wavelength with a Burleigh WA-1500 wavemeter with accuracy better than 100 MHz. The beam was spatially filtered between each cell in order to obtain a smooth axisymmetric quasigaussian transverse profile of FWHM $r_p=2$ mm, but also to maintain amplified spontaneous emission (ASE) at a low level ($\sim 1\%$). Measurements of the energy distribution and of the spatial phase showed that the beam was nearly TEM_{00} (spatial phase was inferred from three intensity measurements at three different propagation distances according to a method detailed in Refs. [8] and [9]). The temporal profile was nearly gaussian with a FWHM of about $\tau=6$ ns.

The atomic medium was generated heating solid europium in a temperature controlled heat pipe oven of 80 cm effective length. A buffer gas (argon) was used to ensure window protection. Argon was held at a low pressure (<1 Torr) in order to maximize the dephasing collision time T_{col} (we measured that 1 Torr of argon led to $T_{col} \approx 170$ ns). At typical working temperatures ($T \approx 650\,^{\circ}$C), the Eu atomic density given by the well-known vapor pressure law [10] was $N \approx 1.510^{14}$ atoms/cm^3 and the Doppler broadening was of the order of 1 GHz.

Natural europium consists in a balanced mixture of two stable isotopes, ^{151}Eu and ^{153}Eu. The laser frequency was tuned in our experiment on the red side of the ^{153}Eu $J=7/2 \rightarrow J=7/2$ transition at 576.5 nm. The corresponding mean (quadratic) electric dipole moment is $\mu=0.47D$ [11]. The $J=7/2 \rightarrow J=7/2$ transition of ^{151}Eu and ^{153}Eu are separated by 3.5 GHz. The hyperfine structure width does not exceed 300 MHz.

Characterization of the emerging pulse was performed in the imaged output plane of the active medium using an Imacon 500 streak camera. This camera was equipped with an intensifier whose image was made with a charge-coupled camera. The imaging system was synchronized with the pulsed light source in order to work in a single shot mode.

Figure 1 compares the spatiotemporal profiles of the light pulse at the entrance of the medium (top) and after a 80 cm propagation in the atomic medium (bottom). The laser was

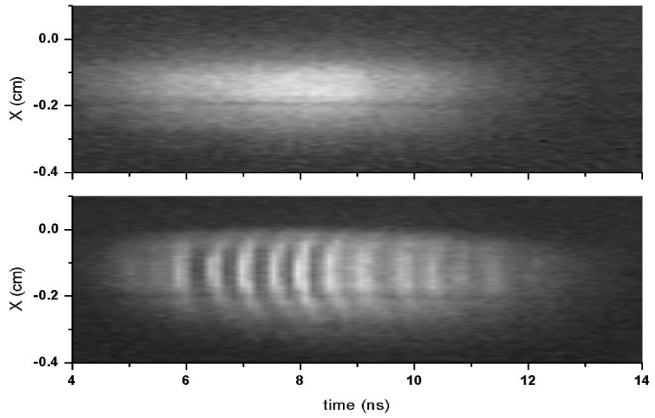

FIG. 1. Streak views of the input (top) and final pulses (bottom). The optical density of the atomic medium was $N\times L \simeq 1.2\,10^{16}$ atoms/cm^2. The slight curvature of the successive temporal slits is due to a small intensity-dependent correction to the pulse velocity [see last term on the right-hand side of Eq. (6)].

detuned from the ^{153}Eu $J=7/2\rightarrow J=7/2$ transition by an amount $\Delta=\omega_L-\omega_{12}=-5.2$ GHz, where ω_{12} is the frequency of the atomic transition. The initial maximum Rabi frequency was equal to 2.8 GHz. In Fig. 1 (bottom) the pulse has propagated into the medium and has undergone strong temporal reshaping, reaching a stage just prior to complete splitting (See below Fig. 3 for $L=120$ cm). Figure 2 shows the on-axis temporal profile and its Fourier transform for the final pulse. The growth of frequency-shifted modes located at $\omega\approx\omega_L\pm 2$ GHz is exhibited.

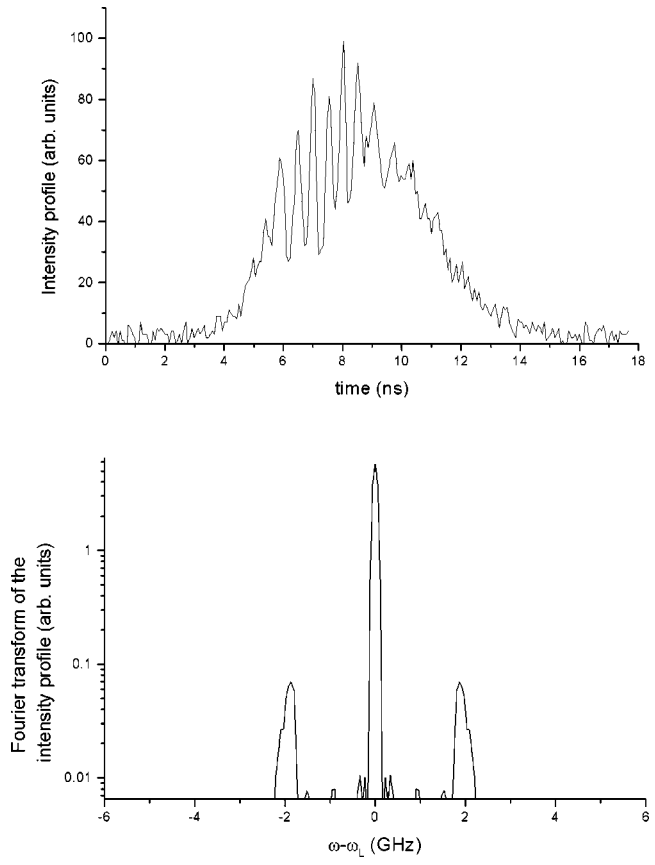

FIG. 2. On-axis temporal profile for the final pulse (top) and corresponding Fourier transform (bottom) ($N\times L \simeq 1.2\,10^{16}$ atoms/cm^2).

III. MAXWELL-BLOCH SIMULATIONS

Two-dimensional axisymmetric Maxwell-Bloch (MB) simulations were run for the interaction conditions met in the experiments. The hyperfine structure of Eu was neglected in our calculations since the corresponding width (<300 MHz) is much lower than the 1 GHz Doppler broadening. The presence of ^{151}Eu was also not taken into account in the simulations. Plane-wave MB simulations not reported here indeed indicated that the off-resonant interaction with isotope ^{151}Eu led only to minor corrections to the temporal reshaping of the input pulse. A white-noise component was added in the input pulse, the amplitude of which was $\epsilon=1\%$ of the input field amplitude. This noise component accounts for the small amount of ASE in our experiment.

Figure 3 shows the evolution of the on-axis temporal profile of the laser pulse for increasing propagation distances L. Strong temporal reshaping is observed and finally leads to pulse splitting for large propagation distances ($L>100$ cm). Figure 4 shows the Fourier transform of the on-axis intensity profile for $L=80$ cm. Pulse splitting appears to be a direct consequence of sideband amplification at $\omega\approx\omega_L\pm 2$ GHz in agreement with the experimental data displayed in Fig. 2.

IV. PERTURBATIVE ANALYSIS

To get a qualitative understanding of the physical processes involved in these results, we start with the MB equations describing the propagation of a slowly varying field envelope E through a collection of two-level atoms. Defining a dimensionless time $\tau=\tau/\tau_p$, field $e=\mu E\tau_p/\hbar$, laser

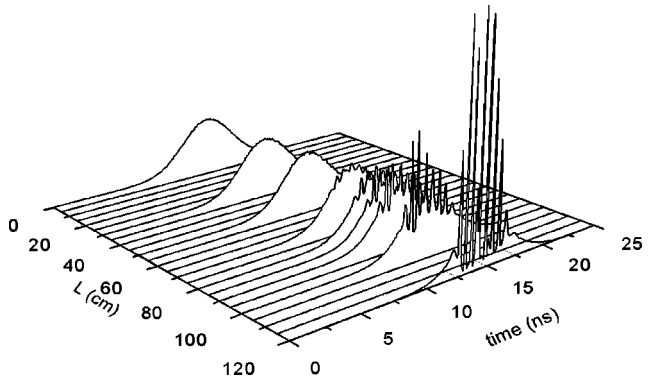

FIG. 3. Calculated evolution of the on-axis temporal profile of the laser pulse as a function of the propagation distance. A white-noise component was added in the input pulse, the amplitude of which was 1% of the input field amplitude. For more details about the interaction conditions, see the main text.

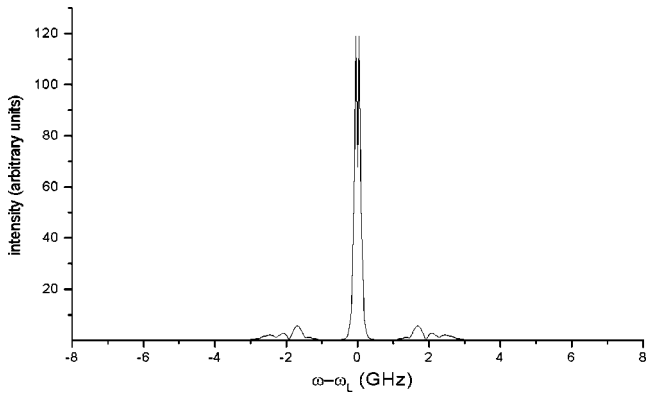

FIG. 4. Fourier transform of the calculated on-axis intensity profile for $L=80$ cm (see Fig. 4 for the corresponding profile in the time domain).

detuning $\delta=2\pi\times\Delta\times\tau_p$, length $\eta=z/L_0$, and gain $g=\omega_L N\mu^2\tau_p L_0/(2\varepsilon_0 c\hbar)$ (where τ_p and L_0 are, respectively, a characteristic pulse time and a characteristic length) the paraxial MB equations are

$$\partial_\eta e+iF\Delta_\perp e=-igp, \tag{1}$$

and

$$\partial_\tau p=-i\delta p+ieW, \tag{2}$$

$$\partial_\tau W=\mathrm{Re}(e\overline{p}). \tag{3}$$

p and W are, respectively, the atomic coherence (related to the slowly varying atomic polarization P through $P=2N\mu p$) and population inversion. The parameter F is the inverse of the Fresnel number, $F=\lambda L/4\pi r_p^2$, where r_p is the beam radius and λ the laser wavelength.

The atomic coherence p can be formally separated into linear and nonlinear parts, $p=p_L+p_{NL}$. The linear contribution to p can be inferred forcing $W=-1$ in Eq. (2). Taking the Fourier transform of the resulting equation, the linear susceptibility $\chi(\omega)$ can be expanded into a Taylor series about ω_L [$\chi(\omega)$ is defined from the envelopes p_L and e through the relation $p_L(\omega-\omega_L)=\varepsilon_0\chi(\omega)e(\omega-\omega_L)$]. Termination of the series after the second term and back transformation into the time domain yield for the linear polarization p_L,

$$p_L=-\frac{e}{\delta}-\frac{i}{\delta^2}\partial_\tau e+\frac{1}{\delta^3}\partial_\tau^2 e. \tag{4}$$

The nonlinear contribution to p can be estimated using the second-order quasiadiabatic approximation given in Ref. [12] in the limit of moderate applied fields (i.e., $|e|^2/\delta^2\ll 1$):

$$p_{NL}=\frac{1}{2\delta^3}|e|^2e+\frac{3i}{2\delta^4}|e|^2\partial_\tau e. \tag{5}$$

Finally, Eq. (1) reduces to

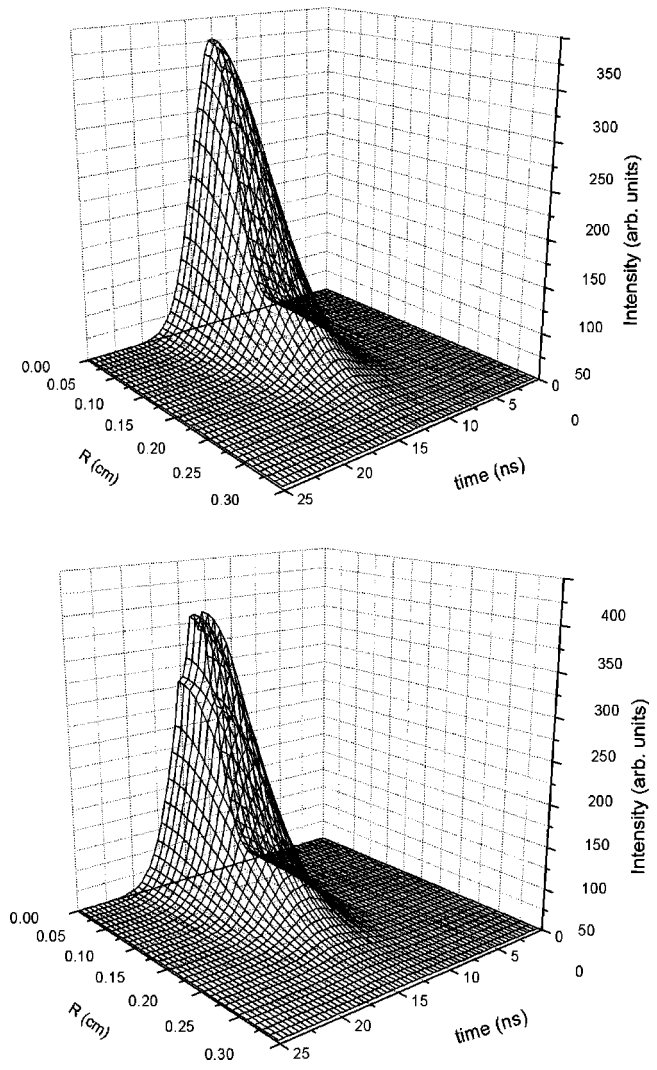

FIG. 5. Calculated spatiotemporal profile for $L=0$ (top) and $L=70$ cm (bottom). For $L=70$ cm (region of initial growth of the modulational instability) the spatial profile is almost left unchanged.

$$\partial_\eta e+iF\Delta_\perp e=\frac{ig}{\delta}e-\frac{g}{\delta^2}\partial_\tau e-\frac{ig}{\delta^3}\partial_\tau^2 e, \tag{6}$$

$$-\frac{ig}{2\delta^3}|e|^2e+\frac{3g}{2\delta^4}|e|^2\partial_\tau e.$$

The last term on the right-hand side of Eq. (6) is responsible for an intensity-dependent correction to the pulse velocity in our experimental conditions and will not be considered further.

Setting

$$e=s\exp\left(\frac{ig}{\delta}z\right), \tag{7}$$

Eq. (6) becomes

$$\partial_\eta s + iF\Delta_\perp s = -\frac{ig}{\delta^3}\partial^2_{\tau'} s - \frac{ig}{2\delta^3}|s|^2 s, \tag{8}$$

where τ' is the retarded time, $\tau' = \tau - g/\delta^2\eta$. Finally, Eq. (8) is the well-known nonlinear Schrödinger equation and describes for $\delta<0$ beam defocusing in a cubic medium (the nonlinear index of refraction of which is $n_2 = N\mu^4/4\hbar\varepsilon_0\delta^3 < 0$) in the regime of normal GVD ($k'' = d^2k/d\omega^2 = -k_0 N\mu^2/\hbar\varepsilon_0\delta^3 > 0$). Neglecting transverse effects (see the concluding remark at the end of this section), it has been shown [13] that the cw solution s_0 of Eq. (8) is unstable for a small perturbation (or modulation) s_1, where $|s_1| \ll |s_0|$ and $s_1 \propto \exp(i\Omega t)$, as a result of the interplay between GVD ($\propto i\partial^2_{\tau'} s$) and SPM ($\propto i|s|^2 s$). Maximum amplitude growth occurs at $\Omega_{max} = \omega_L \pm \Omega_m/\sqrt{2}$. In our experiment, the maximum Rabi frequency Ω_m was almost constant before the splitting stage, i.e., $\Omega_m/\sqrt{2} \simeq cst \simeq 2$ GHz. Thus, this simple analysis predicts that MI sidebands are expected to be roughly located at $\omega_{MI} = \omega_L \pm 2$ GHz, in close agreement with our experimental and numerical results (see Figs. 2 and 4).

The analytical treatment mentioned above is only valid in the linear growth region of perturbations, where the amplitude of modulation s_1 is much smaller than the amplitude of the electric field s_0. From Fig. 3, this is roughly verified for $L \leqslant 70$ cm. In these early stages of propagation, the transverse profile of the pulse does not significantly evolve (see Fig. 5) and diffraction can be ignored when determining the preferentially amplified frequencies.

V. DISCUSSION

The growth of the MI requires initial spectral feed at the amplified frequencies. In our experiment, MI more likely started from a weak noise component in the input pulse than from SPM-induced spectral broadening (setting $\epsilon = 0$ in our simulations inhibits MI). This can be readily understood disregarding diffraction and dispersion in Eq. (8). Thus

$$\partial_\eta s = -\frac{ig}{2\delta^3}|s|^2 s \tag{9}$$

and

$$s(\eta,\tau) = s(0,\tau)\exp[-i\varphi(\eta,\tau)] \tag{10}$$

where

$$\varphi(\eta,\tau) = \frac{g}{2\delta^3}|s(0,\tau)|^2\eta. \tag{11}$$

As seen from Eqs. (10) and (11), SPM spectral broadening—given by the maximum value of $\partial_\tau\varphi(\eta,\tau)$—is linearly proportional to the propagation distance. For the initial pulse gaussian in time $s(0,\tau)$ corresponding to our experiment, one finds that SPM spectral broadening is only 20 MHz for $L = 80$ cm.

Sideband generation in the course of laser propagation has been extensively discussed in the context of conical emission (CE), a topic that has attracted considerable attention for more than two decades [14–16]. In related experiments, propagational FWM of Rabi sidebands—i.e., generated in the vicinity of the time-varying generalized Rabi frequencies $\Omega' = \omega_L \pm (\Omega^2 + \Delta^2)^{1/2}$—has often been exhibited [17–21]. Other works, including the present one, report experimental observation [22] or numerical exhibition [23] of sideband generation at a distinctly different frequency from Ω' [24]. We now briefly discuss that point.

As already pointed out in Refs. [25] and [26], in most of the experiments where sideband generation in the vicinity of Ω' was reported, the incident laser beam has broken up into many self-trapped filaments, resulting in ratios $(\Omega/\Delta)^2$ greater than two. Conversely, in the present paper, but also Ref. [23], the input field strength is such that $(\Omega/\Delta)^2 \simeq 0.25$. Sideband generation appears to originate from distinct processes in these two regimes. Under strong applied field conditions, any broadband background radiation can be amplified by a FWM process. This leads to an intense radiation located in the vicinity of the maximum of the time-varying generalized Rabi frequency [27]. For moderate applied fields (regime probed here but also in Ref. [23]), Ω' is not significantly detuned from the atomic transition frequency [i.e.,$(\Omega^2 + \Delta^2)^{1/2} \simeq \Delta$]. As a consequence, resonant absorption strongly competes with FWM at Ω' and MI is likely to become the leading process of sideband generation.

VI. CONCLUSIONS

To summarize, we have observed MI in the regime of normal dispersion in a slightly defocusing atomic medium. The absolute value of the measured modulation period is in close agreement with numerical and analytical predictions. This fundamental FWM process causes complete pulse splitting. For moderate applied laser fields ($\Omega^2/\Delta^2 \ll 1$), MI may represent the dominant mechanism of sideband generation in the course of near resonant propagation in atomic vapors.

[1] K. Tai, A. Hasegawa and A. Tomita, Phys. Rev. Lett. **56**, 135 (1986).

[2] K. Tai *et al.*, Appl. Phys. Lett. **49**, 236 (1986).

[3] G. Millot, E. Seve, and S. Wabnitz, Phys. Rev. Lett. **79**, 661 (1997).

[4] P. Sprangle, E. Esarey, and B. Hafizi, Phys. Rev. Lett. **79**, 1046 (1997).

[5] P. Sprangle, E. Esarey, and B. Hafizi, Phys. Rev. E **56**, 5894 (1997).

[6] G.P. Agrawal, *Nonlinear Fiber Optics* (Academic Press, New York, 1989).

[7] D.S. Bethune, Appl. Opt. **20(11)**, 1897 (1981).

[8] F. Roddier and C. Roddier, Appl. Opt. **30(11)**, 1325 (1991).

[9] L. Bruel and J. Belledent, ''MIROMA B 12955.3PR'' Patent 02-98 CEA/COGEMA.

[10] A.N. Nesmeyanov, *Vapour Pressure of the Chemical Elements*

(Elsevier, New York, 1963), p. 248.
[11] D. L'Hermite *et al.*, Opt. Commun. **155**, 270 (1998).
[12] M.E. Crenshaw and C.D. Cantrell, Phys. Rev. A **37**, 3338 (1988).
[13] A. Hasegawa and W.F. Brinkman, IEEE J. Quantum Electron. **16**, 694 (1980).
[14] For a review of the theoretical and experimental studies on conical emission prior to 1989, see M.E. Crenshaw and C.D. Cantrell, Phys. Rev. A **39**, 126 (1989).
[15] W. Chalupczak, W. Gawlik, and J. Zachorowski, Opt. Commun. **99**, 49 (1993).
[16] A. Dreischuh *et al.*, Appl. Phys. B **66**, 175 (1998).
[17] D.J. Harter and R.W. Boyd, Phys. Rev. A **29**, 739 (1984).
[18] Ph. Kupecek *et al.*, Opt. Commun. **56**, 1 (1985).
[19] J.F. Valley *et al.*, Phys. Rev. Lett. **64**, 2362 (1990).
[20] P. Weisman, A.D. Wilson-Gordon, and H. Friedmann, Phys. Rev. A **61**, 053816 (2000).
[21] J. Guo, J. Cooper, and A. Gallagher, Phys. Rev. A **52**, R3440 (1995).
[22] G.L. Burdge and C.H. Lee, Appl. Phys. B: Photophys. Laser Chem. **28**, 197 (1982).
[23] M.E. Crenshaw and C.D. Cantrell, Opt. Lett. **13**, 386 (1988).
[24] Our interpretation of the numerical results obtained in Refs. [12,23] differs somewhat from the one given by the authors themselves. Numerical simulations of near resonant propagation of a focused beam were performed with $\Omega_m = 37GHz (\Omega_m/\sqrt{2} \simeq 26GHz)$ and $\Delta = 60GHz$ (i.e., $\Omega'_m = (\Omega_m^2 + \Delta^2)^{0.5} \simeq 70$ Ghz at $L=0$). A frequency-shifted and angularly displaced peak was observed at $\delta = -32$ GHz and $k_\perp = 1130\ \mathrm{cm}^{-1}$ and was interpreted in terms of transient oscillations at the generalized Rabi frequency (although δ appeared to differ significantly from Ω'_m in their work). In an attempt to fill the gap between their numerical results and prior CE experiments (reporting sideband generation at the exact generalized Rabi frequency), the authors argued: ''A result of the practical restriction to a short pulse length is that very little of the pulse is near the maximum Rabi frequency in our calculation. As a result, the temporal frequency at which sidebands first appear is near the detuning frequency rather than the maximum generalized Rabi frequency.'' However, more recent simulations of short laser-pulse propagation (for which Ω_m/Δ was equal to 2 at $L=0$) showed that the spectrum of the final pulse contained the expected frequency sidebands located in the vicinity of Ω'_m (see Ref. [21]). This tendency was also confirmed by our own MB simulations, the pulse duration and the ratio Ω_m/Δ being continuously varied (we will present this parametric study in a separate publication). In fact, considering the laser-matter interaction regime probed in Ref. [23] ($\Omega_m/\Delta \simeq 0.5$, as in our experiment) we believe that the physical process responsible for sideband generation in this earlier work was more likely MI rather than transient oscillations at Ω'_m (note that $\Omega_m/\sqrt{2} \simeq \delta$ in Ref. [23]). Nonlinear self-phase modulation of the focused beam provided the necessary initial spectral feed for the growth of the instability in these simulations.
[25] B.D. Paul *et al.*, Phys. Rev. A **59**, 4784 (1999).
[26] M.L. Dowell *et al.*, Phys. Rev. A **53**, 1775 (1996).
[27] R.W. Boyd *et al.*, Phys. Rev. A **24(1)**, 411 (1981).